

2018

Negative Effect of Calcination to Catalytic Performance of Coal Char-loaded TiO₂ Catalyst in Styrene Oxidation with Hydrogen Peroxide as Oxidant

Mukhamad Nurhadi, *Universitas Mulawarman*

Ratna Kusumawardani, *Universitas Mulawarman*

Hadi Nur, *University Technology Malaysia*

Research Article

Negative Effect of Calcination to Catalytic Performance of Coal Char-loaded TiO₂ Catalyst in Styrene Oxidation with Hydrogen Peroxide as Oxidant

Mukhamad Nurhadi^{1*}, Ratna Kusumawardani¹, Hadi Nur²

¹Department of Chemical Education, Universitas Mulawarman, Kampus Gunung Kelua, Samarinda, 75119, East Kalimantan, Indonesia

²Centre for Sustainable Nanomaterials, Ibnu Sina Institute for Scientific and Industrial Research, Universiti Teknologi Malaysia, 81310 UTM Skudai, Johor, Malaysia

Received: 20th April 2017; Revised: 8th September 2017; Accepted: 8th September 2017;
Available online: 22nd January 2018; Published regularly: 2nd April 2018

Abstract

The research of negative effect of calcination to catalytic performance of coal char-loaded TiO₂ catalyst in styrene oxidation with hydrogen peroxide as oxidant has successfully done. The effects of calcination step to catalyst properties were characterized with Fourier Transform Infra Red (FTIR), X-ray Diffraction (XRD), nitrogen adsorption, Field Emission Scanning Electron Microscopy (FESEM), and Transmission electron microscopy (TEM). The catalytic performance of the catalysts has been investigated in styrene oxidation with hydrogen peroxide as oxidant. The catalytic study showed the calcination step influenced to catalytic properties and could decrease the catalytic performance of coal char-loaded TiO₂ catalyst in styrene oxidation. Copyright © 2018 BCREC Group. All rights reserved

Keywords: Styrene; Oxidation; Calcination; Hydrogen peroxide

How to Cite: Nurhadi, M., Kusumawardani, R., Nur, H. (2018). Negative Effect of Calcination to Catalytic Performance of Coal Char-loaded TiO₂ Catalyst in Styrene Oxidation with Hydrogen Peroxide as Oxidant. *Bulletin of Chemical Reaction Engineering & Catalysis*, 13 (1): 113-118 (doi:10.9767/bcrec.13.1.1171.113-118)

Permalink/DOI: <https://doi.org/10.9767/bcrec.13.1.1171.113-118>

1. Introduction

The preparation of catalyst consists of many steps. Calcination is one of the steps in catalyst preparation. The calcination process was aimed to decompose the metal precursor to form oxide, to modify the texture through sintering and the structure active phase generation, to stabilize of mechanical properties and to remove of gaseous products [1]. Catalytic properties and metal dispersion were very influenced the calcination

temperature, the optimal temperature calcination about 400-500 °C. The temperature calcination above the optimum temperature leads to oxide of active site mobile on the surface and sinter with each other [2].

Indonesia is one of country in the world which produced coal. Coal reserves are found in almost all Indonesia islands which predicted around 21.13 billion short tons. Coal is one of materials which can be considered as particular precursor for production of carbonaceous solids. Carbon from coal can be used as catalyst support and molecular sieve. Many researches have been done to investigate calcination effect

* Corresponding Author.
E-mail: nurhadi1969@yahoo.co.id (Nurhadi, M.)

to catalytic performance such as the effect of the calcination temperature on the performance of a CeMoO_x catalyst in the selective catalytic reduction of NO_x with ammonia [3], the effect of calcination temperature on catalytic performance of CuCe/AC catalysts for oxidative carbonylation of methanol [4], the effect of calcination temperature on stability and activity of $\text{Ni/MgAl}_2\text{O}_4$ catalyst for steam reforming of methane at high pressure condition [5], the hydrogen production from ethanol over Ir/CeO_2 catalyst: Effect of the calcination temperature [6], the effect of calcination conditions on the structure and catalytic performance of MgO supported Fe-Co-Ni catalyst for CO hydrogenation [7], the effect of calcination and metal loading on the characteristics of Co/NaY catalyst for liquid-phase hydrogenation of ethyl lactate to 1,2-propanediol [8], and the effect of calcination temperature on the catalytic activity of VPO for aldol condensation of acetic acid and formalin [9]. Previous researches concluded that calcination process can cause the physico-chemical properties, the activity and stability of the catalyst change. Due to the properties of coal char is sensitive to temperature so that the calcination temperature should be maintained at certain level particularly when the coal char was used as catalyst support.

In this research we have investigated the influence of calcination step in preparation of coal char loaded TiO_2 catalyst for oxidation of styrene with aqueous hydrogen peroxide as oxidant. We found that the calcination process give negative effect to catalytic performance of catalyst in oxidation of styrene with aqueous hydrogen peroxide.

2. Materials and Methods

2.1 Catalyst preparation

The coal was known from low rank coal precisely as lignite which obtained from Kutai Kartanegara East Kalimantan, Indonesia [10]. The coal char was obtained by pyrolysis of the coal sample in a fluidized bed unit under the nitrogen atmosphere by using gas flow rate 100 cc/min, at 600 °C for 2 h, and by heating rate 5 °C/min. The coal char (CC600) was sulfonated by adding 12 mL of 98% sulfuric acid (JT Beker) per gram of coal, stirring and heating in an oil bath at 90 °C for 6 h. The sulfonated coal char (SCC600) will be obtained after the coal char was washed with warm distilled water at 80 °C to remove sulfate ions, and it was dried at 110 °C for overnight. Furthermore, the

sulfonated coal char (SCC600) was impregnated with titanium tetra-isopropoxide (97 %, Aldrich, 500 $\mu\text{mol.g}^{-1}$) in toluene by vigorous stirring at room temperature until toluene completely evaporated. Then, the solid was washed with ethanol and dried at 110 °C to remove toluene. The catalyst that obtained was labeled TiSCC600.

The calcination process for the catalyst TiSCC600 was carried out in a stainless steel reactor in a vertical furnace under nitrogen atmosphere at 500 °C with heating rate of 5 °C/min and maintained for 2 h. The catalyst was labeled as Ca/TiSCC600 .

2.2 Samples characterization

XRD patterns of the catalysts were recorded with a Bruker AXS Advance D8 diffractometer using $\text{Cu-K}\alpha$ radiation ($\lambda = 1.5405 \text{ \AA}$, 40 kV and 40 mA). IR spectra of the catalysts were collected on a Perkin Elmer Fourier transform infrared (FTIR) spectrometer, with a spectral resolution of 2 cm^{-1} , scans 10 s, at temperature 20 °C. The BET surface area of the catalysts was measured by N_2 adsorption at 77 K using a Micromeritics ASAP 2020 V4.00. The Barrett-Joyner-Halenda (BJH) model was used to evaluate the pore size distribution. The surface textures in the catalysts were obtained by using field emission scanning electron microscopy (FESEM), JEOL JSM-6701F instrument with an accelerating voltage of 15 kV. The images of Transmission electron microscopy (TEM) were recorded with a JEOL JEM-2100 electron microscope operated at an accelerating voltage of 200 kV and connected with a Gatan 794 CCD camera.

2.3 Catalytic activity test

The oxidizing styrene using 30% aqueous H_2O_2 as oxidant was used to catalytic testing of catalyst. The catalytic tests were carried out according to the modification procedure reported previously [11]. All reactions were carried out at room temperature with mixing styrene (5 mmol), 30 % aqueous H_2O_2 (5 mmol), acetonitrile (4.5 mL), and catalyst (50 mg) with stirring for 20 h. The reaction products were analyzed by GC-2014 Shimadzu.

3. Results and Discussion

3.1 Physical properties

Figure 1 shows the XRD pattern of TiSCC600 and Ca/TiSCC600 . Both of the solid catalysts show peak at $2\theta = 26.5^\circ$ which is indicated to quartz crystalline structure

[12,13]. Base on JSPDF number 00-004-0477, both solid catalysts possess anatase titania crystalline structure which can be shown of peaks at $2\theta = 25.4, 37.9, \text{ and } 55.1^\circ$. Calcination process at 500°C for 2 h was not influenced to the anatase crystalline structure of titania. Previous studies have proven that pure anatase will be converted to rutile above around 500°C at slow rate [14].

Figure 2 shows the FTIR spectra for TiSCC600 and Cal/TiSCC600. The IR absorption a broad peak at around 3429 cm^{-1} due to O–H stretching mode of the –COOH and phenolic OH groups [15]. The intensity of OH groups decreased after TiSCC600 was calcined. Calcination process caused the appearance of peaks at around 2926 and 2851 cm^{-1} that attributed to symmetric and asymmetric stretching mode of the C–H sp^3 groups and correlated the peak at 1462 cm^{-1} was attributed as bending mode of C–H [16]. The peak at around 1094 cm^{-1} was attributed to the asymmetric stretching of Si–O–Si groups also appear after calcination process. Both solid catalysts spectra show an adsorption band in the 965 cm^{-1} , this band can be considered the fingerprint of the existence of framework titanium and correlated the peak at around 469 cm^{-1}

cm^{-1} was indicated to the symmetric O–Ti–O stretching that caused the vibration of Ti–O bond.

Figure 3 shows N_2 adsorption-desorption isotherms and pore size distributions of TiSCC600 and Cal/TiSCC600. Both isotherms show the typical V type isotherms in the IUPAC classifications of mesoporous materials with clear hysteresis loops in the relative pressure range $\sim 0.14 - 0.995$ (TiSCC600) and $\sim 0.17 - 0.997$ (Cal/TiSCC600), which are due to the capillary condensation of nitrogen in the pores. In addition, both samples possess another type H3 hysteresis loops which is characteristic of agglomerates of particles forming slit shape pores with nonuniform size and shape [17]. Physical properties of TiSCC600 and Cal/TiSCC600 samples are listed in Table 1. The pore size distribution indicates the presence of uniform mesopores $\sim 197\text{ \AA}$ (TiSCC600) and $\sim 422\text{ \AA}$ (Cal/TiSCC600). Compared with the pore sizes of TiSCC600, the pore size of Cal/TiSCC600 increase obviously, this is caused opening and collapsing of pores during calcination process.

Field emission scanning electron microscopy was used to collect information about catalysts morphology. A representative FESEM

Table 1. Physical properties of catalysts

Samples	BET Surface Area [21]	Pore Volume (cm^3/g)	Average Pore Size (\AA)	Micropore volume (cm^3/g)
TiSCC600	18.42	0.052	105.4	0.0004
Cal/ TiSCC600	4.00	0.003	422.9	0.0003

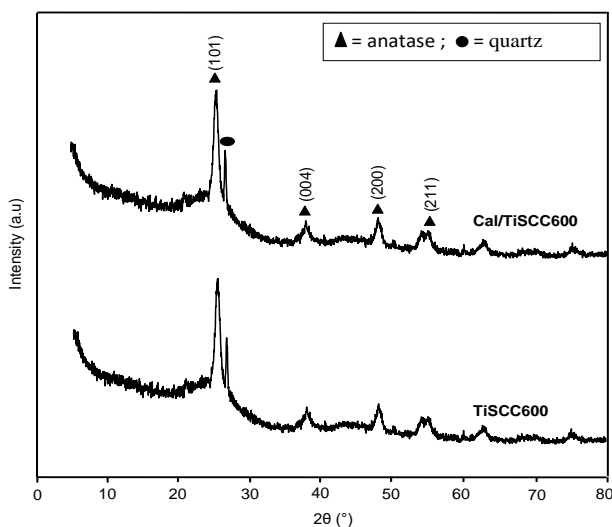


Figure 1. XRD pattern of TiSCC600 and Cal/TiSCC600

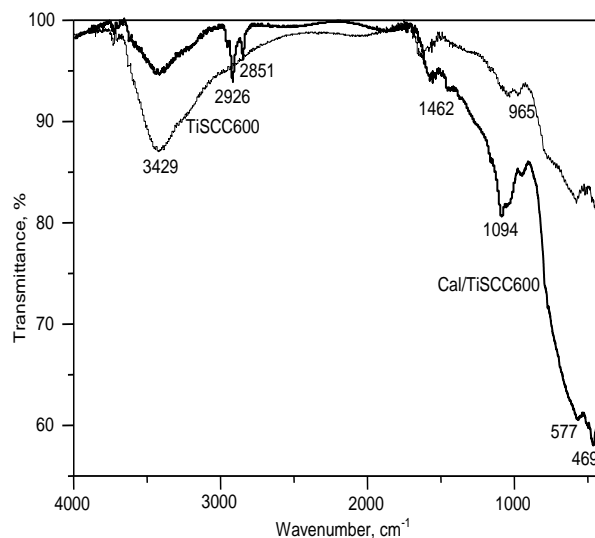


Figure 2. FTIR spectra of TiSCC600 and Cal/TiSCC600

micrograph of TiSCC600 and Cal/TiSCC600 are shown in Figure 4. Compared with the micrograph of Cal/TiSCC600, TiSCC600 possesses morphology more roughness than Cal/TiSCC600. This due to titania agglomeration has collapsed and immersed inside SCC600 surface which to be soft during calcination process.

Figure 5 shows the TEM image of TiSCC600, which is in good agreement with XRD result, mainly due to the titania agglomeration on the SCC600 surface. Image is similar to that along the (101) direction. The crystallinity of titania in anatase phase can be observed by crystal lattice planes with d-spacing of 0.31 nm for the plane (101).

3.2 Catalytic activity test results

The effect of calcination process to catalytic performance can be investigated by styrene oxidation with TiSCC600 and Cal/TiSCC600 as catalysts. The yields of products from catalytic performance test can be shown in Figure 6. Benzaldehyde, phenyl acetaldehyde, and styrene oxide were as dominant products in oxidation of styrene with H₂O₂ as an oxidant. It is observed that the yield of benzaldehyde was 0.821 mmol with TiSCC600 as catalyst and the yield drastically decrease to 0.029 mmol when Cal/TiSCC600 was used as catalyst. This due to titania phase anatase which isolated in tetrahedral form that considered as the most active in oxidation reaction underwent change shape and start to be converted to rutile phase when calcined above 465 °C. Calcination

process also causes the collapse of the porous structures of titania and SCC600. The evident can be shown in Table 1, TiSCC600 before calcination has BET surface area and micropore volume higher than Cal/TiSCC600. SCC600 from coal has properties to be soft when it heated at about 400 °C, so titania as active site become inactive due to immersed inside of SCC600's soft surface [18]. Base on FTIR result, the decreasing of yield also was caused by the releasing of OH groups from the catalyst surface that have a role as the Brønsted acid sites. The Brønsted acid sites in oxidation of styrene can support to form benzaldehyde as product.

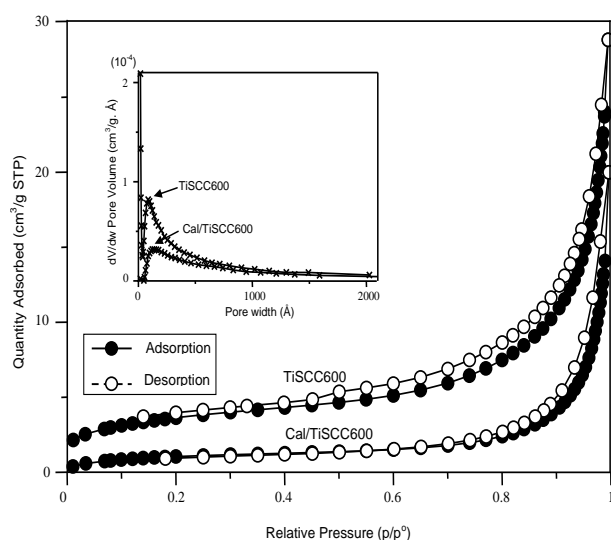


Figure 3. BET Surface Area of TiSCC600 and Cal/TiSCC600

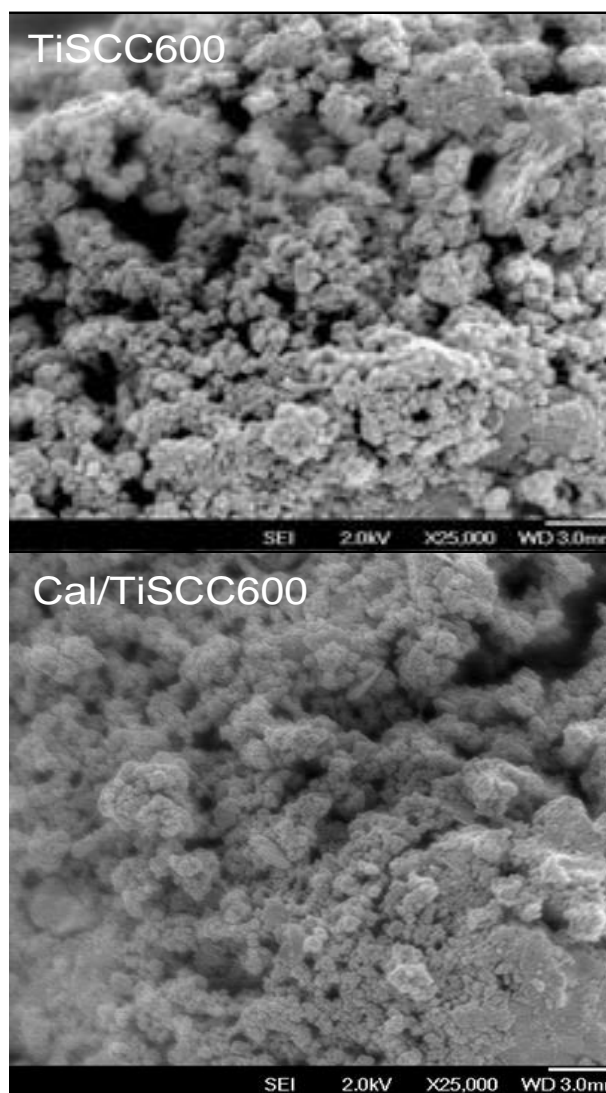


Figure 4. FESEM images of TiSCC600 and Cal/TiSCC600

4. Conclusions

The effect of calcination step in catalyst preparation has been studied. The catalytic activity of coal char-loaded TiO₂ catalyst (TiSCC600) without calcination step in the oxidation of styrene higher than catalyst (Cal/TiSCC600) which calcined. The calcination process during catalyst preparation can cause surface area of catalyst decrease, the releasing of the Brønsted acid sites from the catalyst surface and the titania (TiO₂) active site become inactive.

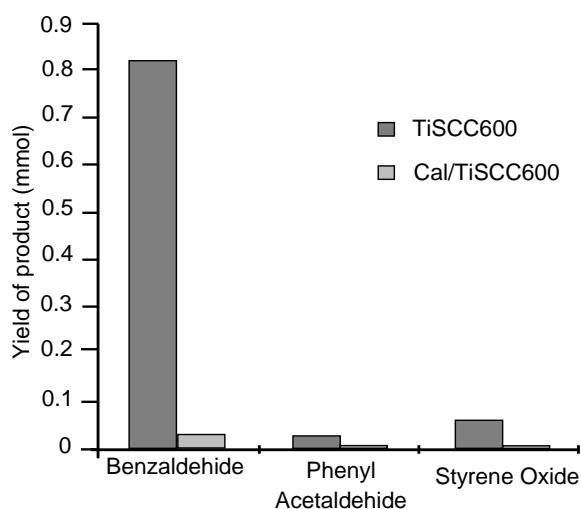


Figure 6. Comparison of catalytic activity of TiSCC600 and Cal/TiSCC600 in the oxidation of styrene (5 mmol), 30% H₂O₂ (5 mmol) and catalyst (50 mg). The yield of product at room temperature for 20 h

Acknowledgements

The author is grateful to the support of dean of Education Faculty, Universitas Mulawarman, East Kalimantan, Indonesia.

References

- [1] Perego, C., Villa, P. (1997). Catalyst preparation methods. *Catal. Today*, 34(3-4): 281-305.
- [2] Pinna, F., (1998). Supported metal catalysts preparation. *Catal. Today*, 41(1-3): 129-137.
- [3] Jihui, W., Xuesong, D., Yujie, W., Yongdan, Li. (2015). Effect of the calcination temperature on the performance of a CeMoOx catalyst in the selective catalytic reduction of NOx with ammonia. *Catal. Today* 245: 10-15.
- [4] Zhang, G., Guo, T., Zheng, H., Li, Z. (2016). Effect of calcination temperature on catalytic performance of CuCe/AC catalysts for oxidative carbonylation of methanol. *J. Fuel Chem. Technol.*, 44(6): 674-679.
- [5] Sanjay, K., Abhishek, G., Goutam, D., Deepak, K. (2016). Effect of calcination temperature on stability and activity of Ni/MgAl₂O₄ catalyst for steam reforming of methane at high pressure condition. *Int. J. Hydrogen Energy* 41: 14123-14132.
- [6] Jie, Z., Bo, Y., Shaoyin, Z., Jianghua, Z., Yongdong, C., Li, C., Tongkuan, X., Weijie, C. (2015). Hydrogen production from ethanol over Ir/CeO₂ catalyst: Effect of the calcination temperature. *Fuel* 159: 741-750
- [7] Hasan, O. T., Samaneh, V., Ali, A. M. (2014). Effect of calcination conditions on the structure and catalytic performance of MgO sup-

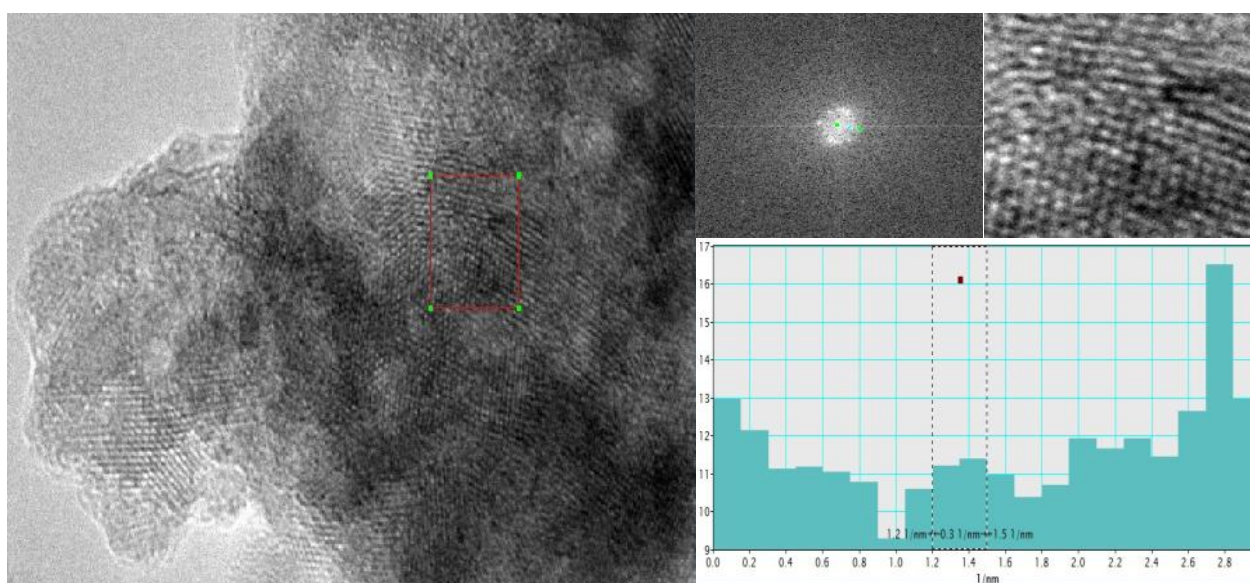


Figure 5. TEM image of TiSCC600

- ported Fe–Co–Ni catalyst for CO hydrogenation. *J. Nat. Gas Sci. Eng.* 17: 110-118.
- [8] Xiaopeng, Z., Hua, W., Xiao, L., Jinyu, H., Xinli, Z., Qingfeng, G. (2016). Effect of calcination and metal loading on the characteristics of Co/NaY catalyst for liquid-phase hydrogenation of ethyl lactate to 1,2-propanediol. *Microporous Mesoporous Mater.* 233: 184-193
- [9] Dan, Y., Chidchon, S., Kenzi, S., Zengxi, L., Chunshan, L. (2016). Effect of calcination temperature on the catalytic activity of VPO for aldol condensation of acetic acid and formalin. *Chem. Eng. J.* 300: 160-168
- [10] Nurhadi, M. (2017). Modification of Coal Char-loaded TiO₂ by Sulfonation and Alkylsilylation to Enhance Catalytic Activity in Styrene Oxidation with Hydrogen Peroxide as Oxidant. *Bull. Chem. React. Eng. Catal.*, 12(1): 55-61.
- [11] Zhan, W., Guo, Y., Wang, Y., Guo, Y., Liu, X., Wang, Y., Lu, G. (2009). Study of Higher Selectivity to Styrene Oxide in the Epoxidation of Styrene with Hydrogen Peroxide over La-Doped MCM-48 Catalyst. *J. Phys. Chem. C*, 113(17): 7181-7185.
- [12] Liu, Y., Chen, J., Yao, J., Lu, Y., Zhang, L., Liu, X. (2009). Preparation and properties of sulfonated carbon–silica composites from sucrose dispersed on MCM-48. *Chem. Eng. J.*, 148(1): 201-206.
- [13] Hasegawa, G., Kanamori, K., Nakanishi, K., Hanada, T. (2010). Fabrication of activated carbons with well-defined macropores derived from sulfonated poly(divinylbenzene) networks. *Carbon.* 48(6): 1757-1766.
- [14] Yu, Y. (2004). Preparation of nanocrystalline TiO₂-coated coal fly ash and effect of iron oxides in coal fly ash on photocatalytic activity. *Powder Technol.*, 146(1-2): 154-159.
- [15] Peng, L., Philippaerts, A., Ke, X., Van Noyen, J., De Clippel, F., Van Tendeloo, G., Sels, B. F. (2010). Preparation of sulfonated ordered mesoporous carbon and its use for the esterification of fatty acids. *Catal. Today.* 150(1-2): 140-146.
- [16] Poh, N.E., Nur, H., Muhid, M.N.M., Hamdan, H. (2006). Sulphated AlMCM-41: Mesoporous solid Brønsted acid catalyst for dibenzoylation of biphenyl. *Catal. Today.* 114(2-3): 257-262.
- [17] Leofanti, G., Padovan, M., Tozzola, G., Venturelli, B. (1998). Surface area and pore texture of catalysts. *Catal. Today*, 41(1-3): 207-219.
- [18] Walker, J. (1986). Coal derived carbons. *Carbon*, 24(4): 379-386.